Kuwait J. Sci. **41** (1) pp. 107-127, 2014

Preparation and characterization of nitrogen doped ZnO films and homojunction diodes

A. E. RAKHSHANI*, A. BUMAJDAD**, J. KOKAJ* AND S. THOMAS*

**Department of Physics, Faculty of Science, Kuwait University, P. O. Box 5969, Safat 13060, Kuwait.*

***Department of Chemistry, Faculty of Science, Kuwait University, P. O. Box 5969, Safat 13060, Kuwait.*

Corresponding Author: ali.rakhshani@ku.edu.kw

ABSTRACT

Nitrogen-doped ZnO (ZnO:N) films were prepared by the reactive magnetron sputtering technique using a zinc target. The effect of thermal annealing in different ambient on the films composition, chemical bonding states, structure, optical transmittance and photoconductivity was investigated. The as-grown films are composed from 9-nm large grains with strained unit cell. The annealing process relaxes the strain and increases the grain size to 39 nm. Annealing also increases the direct band gap of the film from 2.42 eV to 3.26 eV. The as-grown and annealed films show photoconductivity in the visible region which is partly due to the effect of a nitrogen-related defect level with the ionization energy of 1.71 eV. The conversion of the as-grown n-type films to p-type ZnO was achieved by annealing the films in air. The converted p-ZnO and electrodeposited n-ZnO films were used in the fabrication of light-emitting homojunction diodes. Diodes with a reasonably good current-voltage rectification factor exhibited electroluminescence property in the ultraviolet-visible region. From the junction capacitance of these diodes the density of holes in p-ZnO films grown on stainless steel substrates was determined as 1.5×10^{17} cm^{-3}.

Keywords: Composition; homojunction; optoelectronic; XPS; ZnO:N

INTRODUCTION

Zinc oxide is an intrinsically n-type semiconductor with direct band gap of 3.37 eV (300 K) and many interesting characteristics suitable for a wide range of applications (Look, 2005, Ozgur *et al.*, 2005, Pearton *et al.*, 2003). Its large exciton binding energy (60 meV) makes ZnO an efficient material for room-temperature light emitting and lasing devices in the ultraviolate (UV) and visible (defect-related emission) range of spectrum. The main obstacle in the development of ZnO-based homojunction devices is the difficulty in achieving a reliable and stable p-type doping. Nevertheless, some groups have reported the fabrication of diodes showing electroluminescence (EL) property (Nakahara *et*

al., 2010; Kato *et al.*, 2011; Sun *et al.*, 2011; Liu *et al.*, 2012). Synthesizing p-type ZnO remains to be a challenge because of the self compensation effect introduced by the native donor defects like oxygen vacancy (V_O) and zinc interstitial (Zn_i). Atomic nitrogen is an effective p-type dopant in ZnO, likely due to its similar size to oxygen. One technique which has been used widely for the preparation of p-type ZnO is the preparation of zinc nitride, Zn_3N_2, followed by its thermal oxidation (Zou *et al.*, 2009; Wang *et al.*, 2003; Wang *et al.*, 2004; Li *et al.*, 2003; Nakano *et al.*, 2006). In thermal oxidation of Zn3N2, nitrogen is replaced by the ambient oxygen and the residual nitrogen atoms in the transformed ZnO act as acceptors. Zn_3N_2 can be prepared by various techniques including reactive sputtering using a zinc target (Zou *et al.*, 2009; Wang *et al.*, 2003; Yang *et al.*, 2009; Nunez *et al.*, 2012; Zhang *et al.*, 2007). The band gap of Zn_3N_2 films prepared by different techniques is reported to vary between 0.9 eV and 3.4 eV (Khan & Cao, 2010; Paniconi *et al*, 2008). This unusual wide variation is likely caused by the contamination of Zn_3N_2 with oxygen at different levels. Oxygen contamination can occur during the preparation and also during the storage of films in air. A small amount of oxygen in the sputtering chamber can produce effective oxygen incorporation in the film because the Zn-O bond is far more stable than the Zn-N bond. Some recent reports indicate that oxygen can be incorporated unintentionally in Zn_3N_2 films even when the growth takes place in a high vacuum condition (Nunez *et al.*, 2012; Zhang *et al.*, 2007). Out-gassing from the chamber walls induced by plasma action is identified to be one of the plausible sources for oxygen contamination (Nunez *et al.*, 2012).

In this work films were prepared by radio frequency (rf) sputtering technique using a Zn target and nitrogen as the reactive gas. Due to the residual oxygen in the chamber, the films were grown to be nitrogen-doped ZnO (ZnO:N) rather than Zn_3N_2. The optoelectronic properties of this type of ZnO film have not been explored sufficiently. Due to this, the effect of thermal annealing in different ambient on the properties of ZnO:N films was investigated. The conversion of ZnO:N films to p-ZnO by thermal annealing in air and subsequently the fabrication of homojunction devices showing EL property were realized. Here, we report the results of this study.

EXPERIMENTAL

ZnO:N films with a typical thickness of 250 nm were deposited on borosilicate glass substrate (cleaned ultrasonically in ethanol for 10 min) by rf (13.6 MHz) magnetron sputtering (Torr International Inc, model CRC-300) using a zinc target (diameter 51 mm) with purity of 99.99 %. The sputtering was carried out in a N_2/Ar gas mixture. The working pressure was maintained at 2.6 Pa and the

flow rates for Ar and N_2 (both, 99.99% pure) were 8 and 32 cm^3/min, respectively (80% nitrogen in the gas mixture). The chamber was initially evacuated to $5.3x10^{-3}$ Pa and then the mixed gas was introduced through two independently-controlled mass flow meters. The rf power was maintained at 40 W. The substrate (not heated intentionally) was about 7 cm far from the target and rotated at 3.0 rev/min. The rate of deposition (0.12 nm/s) and the film thickness were controlled by a quartz-crystal thickness monitor. Prior to the deposition (opening the shutter), the surface of the target was sputter cleaned for 10 minutes.

The post-deposition thermal annealing was performed in a rapid thermal processor (Annealsys model AS-Micro) at 500°C for 60 minutes in different ambient such as nitrogen and dry air (atmospheric pressure). Annealing at a low nitrogen pressure (105 Pa), which hereafter will be referred to as vacuum annealing, was also performed. Films were characterized by scanning electron microscopy, SEM, (Joel, JSM-6300), x-ray photoelectron spectroscopy, XPS, (VG Scientific 200) and x-ray diffraction, XRD, (Siemens D500) using the CuK_α line (0.15406 nm). A Varian double-beam spectrometer (Cary 5E) was used for the optical transmittance measurements. For the lateral photoconductivity measurements two parallel silver strips with a separation of about 2 mm were deposited on the film surface. A potential difference up to 5V was maintained across the strips and the monochromatic beam of light was incident on the film surface through the gap between the strips. Photocurrent normalized to the incident photon flux was measured at different incident wavelengths, using a setup consisting of a grating monochromator (Sciencetech 9050), lock-in amplifier (Stanford Research SR 530), current amplifier (Keithley 428) and mechanical chopper.

The fabricated devices (see text) were characterized by the means of current-voltage (IV) and capacitance-voltage (CV) measurements using a source-measure unit (Keithley 236) and a CV analyzer (Kiethley 590), respectively. The spectrum of EL emission was recorded using a spectrophotometer (EG&G 1235) equipped with a photodiode array detector (EG&G 1421).

RESULTS AND DISCUSSION

Composition

Figure 1 shows the XPS spectra for the as-grown sample after a surface layer of $\sim$ 24 nm was removed by argon-ion etching. The Zn 2p3 peak at the binding energy (BE) of 1021.1 eV is the characteristic of Zn-O bond in ZnO. A peak with the same BE was also detected before etching the surface.

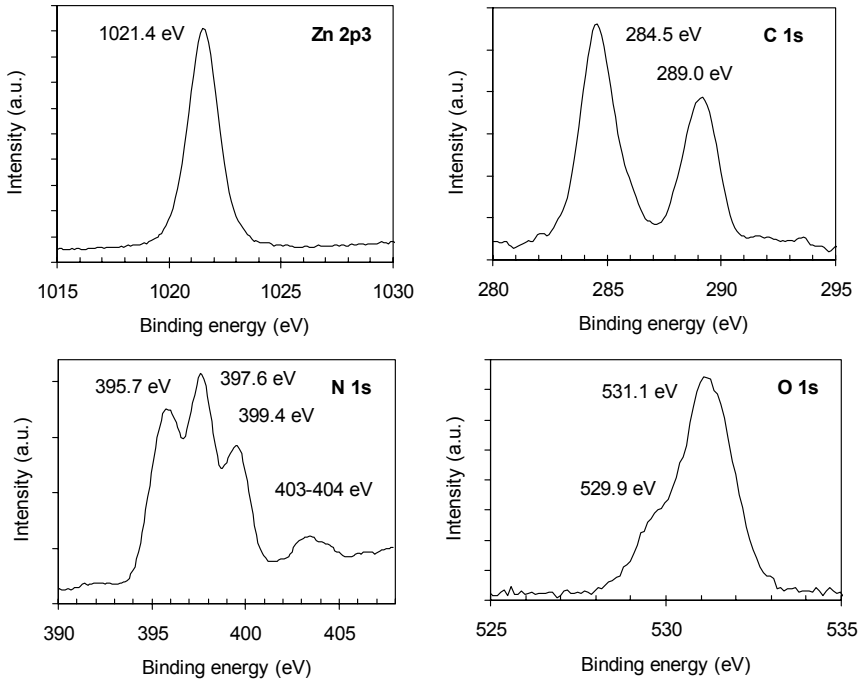

Fig. 1. The XPS spectra for the as-grown film.

The C 1s spectrum shown in Figure 1 consists of two peaks with BE of 284.5 eV and 289.0 eV. The same values were also detected before the etching process. The peak with BE = 284.5 eV is due to the contaminant carbon element and the 289.0-eV peak is the characteristic of the C=O bonds related to organic contaminants (Qureshi *et al.*, 2010). The annealed samples did not show the peak with BE = 289.0 eV due to the thermal dissociation of the organic compounds.

The O 1s spectrum in Figure 1 consists of two peaks. The peak at BE = 529.9 eV represents the O-Zn bond in ZnO and the peak at BE = 531.1 eV is attributed to the loosely bounded O (e.g., O in OH groups) or can be due to the oxygen ions in the oxygen-deficient regions (Djurisic *et al.*, 2007). The O 1s signal detected from the surface of the un-etched sample showed only one peak at BE = 531.1 eV. This implies that the surface of the as-prepared sample is covered with the hydroxide groups, apparently formed due to the exposure of sample to humidity. These hydroxide groups can be removed by the heat treatment of samples as the results of thermal desorption or decomposition.

The N 1s spectrum shown in Figure 1 is composed from four peaks with the BE = 395.7 eV, 397.6 eV, 399.4 eV and 403- 404 eV. The same peaks were also recorded before the argon-ion surface etching. The peak at 395.7 eV is attributed to the N-Zn bond (e.g., in Zn_3N_2) (Zong *et al.*, 2006; Yang *et al.*, 2009; Watanabe *et al.*, 2011). The peak appearing at 397.6 eV has been attributed to the N-H (Watanabe *et al.*, 2011) and also to the N-Zn bonds (Zou *et al.*, 2009). Most likely, it represents a N-Zn bond when N occupies the oxygen vacancy (V_O) site in ZnO to form $(N)_O$ species (Liu *et al.*, 2011; Zhang *et al.*, 2007; Li *et al.*, 2008; Fons *et al.*, 2006; Perkins *et al.*, 2005). The peak appearing at 399.4 eV is the characteristic of the N-C bond (Watanabe *et al.*, 2011) and the small peak at BE = 403- 404 eV is attributed to the $(N_2)_O$ species when N_2 occupies the V_O site (Zhang *et al.*, 2007; Li *et al.*, 2008). The $(N)_O$ defect in ZnO has been assumed by many researchers to be a shallow acceptor with the ionization energy of 170 - 200 meV (Özgür *et al.*, 2005) whereas $(N_2)_O$ behaves as a double donor. The balance between the densities of $(N)_O$ acceptors and donor-type defects like $(N_2)_O$,V_O and Zn_i determines the type of conductivity in ZnO (Li *et al.*, 2008; Fons *et al.*, 2006; Perkins *et al.*, 2005). However, based on some recent theoretical (Lyons *et al.*, 2009) and experimental (Tarun *et al.*, 2011) results it is believed that $(N)_O$ contributes to a deep acceptor level. The shallow acceptor level in p-type nitrogen doped ZnO is likely related to the nitrogen-associated defect complexes.

The XPS-determined Zn/(Zn + O) and N/(Zn + O) atomic ratios for the as-grown film of Figure 1 were 0.45 and 0.07, respectively. The former ratio did not vary considerably as a result of the annealing processes discussed below. However, the latter ratio decreased by a factor of ten indicating the escape of nitrogen from the film. This is in agreement with other reports that the annealing process induces the out diffusion of nitrogen from the $(N_2)_O$ and $(N)_O$ defects to form nitrogen bubbles in the film (Zou *et al.*, 2009; Fons *et al.*, 2006).

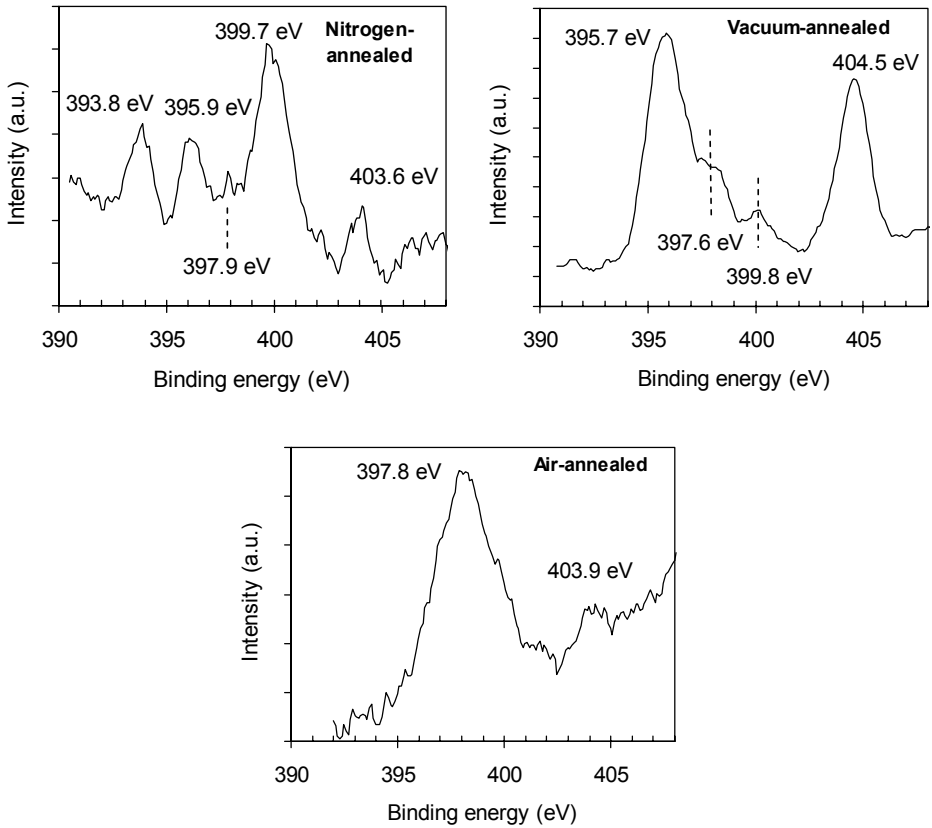

Fig. 2. The XPS N 1s spectra for the annealed films.

The effect of annealing (500 °C, 1 hour) in different ambient on the chemical bonding state of the films was studied. Figure 2 depicts the N 1s spectra for the annealed samples. Annealing in nitrogen slightly increases the density of $(N_2)_O$ and considerably reduces the density of $(N)_O$ defects, as it is evident from the shape of the peaks at 403.6 eV and 397.9 eV, respectively. Nitrogen atoms diffuse out from the $(N)_O$ defects and are replaced by the nitrogen molecules from the annealing ambient. The enhancement of the N-C peak (399.7 eV) is likely due to a chemical reaction between the carbon contaminants of the sample and the nitrogen molecules from the annealing ambient. The annealing process also dissociates the Zn_3N_2 molecules embedded in the sample. This is evident from the smaller size of the peak appearing at 395.9 eV, as compared to that for the as-grown sample (395.7 ev). The O 1s and C 1s signals of the sample annealed in nitrogen (not shown) revealed that the annealing process removes the OH and C=O groups. The peak appearing at 393.8 eV in the spectrum of the nitrogen-annealed sample could not be identified based on the literature data.

For the vacuum-annealed sample, the N 1s spectrum shows an enhancement for both, the 395.7-eV peak (N-Zn bond) and the 404.5-eV peak related to the $(N_2)_O$ defects. In vacuum annealing, oxygen escapes from the lattice creating V_O defects. This is concluded from the O 1s spectrum of the sample (not shown). The O 1s spectrum consisted from a strong peak at BE = 530 eV (O-Zn bonds) and a shoulder at 531.5 eV which can be attributed either to the oxygen deficiency defects or to the OH groups (Djurisic *et al.*, 2007). The latter possibility is unlikely to be the case because annealing removes the OH groups. Since vacuum annealing increases the density of V_O sites, more nitrogen molecules occupy these sites to form $(N_2)_O$ defects. Although the pressure of the ambient nitrogen is low, nevertheless it seems that this process is taking place and leads to the enhancement of the N 1s peak at ˜ 404 eV. Part of the excess Zn produced as a result of oxygen escaping from the lattice reacts with nitrogen to form Zn_3N_2. This leads to the enhancement of the 395.7-eV peak assigned to the N-Zn bond. The vacuum-annealed sample also contains $(N)_O$ (shoulder appearing at 397.6 eV) and other species with the N-C bond. The density of species with the N-C bond (the ridge at 399.8 eV) is considerably lower in this sample than in those annealed in the atmospheric pressure of nitrogen. As mentioned above, part of the excess zinc atoms produced by vacuum annealing reacts with nitrogen and yields zinc nitride. The remaining elemental Zn decreases the film optical transmittance. These films have a darker appearance than the yellow-brown color of the as-grown films. Also, the presence of elemental Zn in the vacuum annealed sample was associated with a 0.3-eV shift of the Zn 2p3 peak to lower values.

The N 1s spectrum of the air-annealed sample exhibits a strong peak with BE = 397.8 eV, corresponding to the acceptor-type $(N)_O$ defects, and a minor peak at 403.8 eV which is attributed to the double-donor $(N_2)_O$ defects. This implies that the air-annealing process increases the density of $(N)_O$ acceptors over that for the double donors. This could possibly explain the result of our measurement that the air-annealed sample is p-type, if $(N)_O$ behaves as a shallow acceptor. For $(N)_O$ acting as a deep acceptor level, the conversion of conductivity type by air annealing is apparently due to the out diffusion of nitrogen from $(N_2)_O$ defects which leads to the percentage content of $(N_2)_O$ to fall below that for the shallow acceptors. The out diffusion of nitrogen from $(N_2)_O$ defects is associated with the increase of the density of V_O donor defects. The role of oxygen in the ambient gas is to suppress the increase of V_O density during the annealing process. It is well known that the n-type to p-type conversion of ZnO:N is possible only in the oxygen-containing ambient.

Structure

The as-grown and annealed films deposited on glass substrate showed a uniform and smooth surface, in contrast to the granular surface morphology of the films

grown on metallic substrates. The XRD patterns for the as-grown and annealed films (Fig. 3) reveal only the diffraction peaks (indexed) corresponding to the hexagonal structure of ZnO. Despite the fact that the films were prepared without intentional heating of the substrate, the as-grown films were crystalline. The films crystallineity was improved with the post deposition annealing process. The extent of improvement was found to depend on the annealing ambient which influences the state of the defects as discussed above, based on the XPS results. Annealing in different ambient did not make a noticeable change in the films surface morphology. The XRD patterns in Figure 3 reveal that the (100) peak is more intensive than the (002) peak. This is in contrast to the (002) preferential orientation which normally is observed for undoped ZnO films grown on amorphous and crystalline substrates. The suppression of the c-axis texturing is apparently related to the effect of nitrogen incorporation in the film. The structural parameters (lattice constants and grain size) of the as-grown and annealed films were evaluated from the XRD peaks. The lattice constant c was determined from the diffraction angle, θ, of the (002) peak and the lattice constant a was obtained from the (100) and (110) peaks using the Bragg equation, $2d\sin\theta = \lambda$. Here, λ (= 0.15406 nm) is the wavelength used and d is the spacing of the diffraction planes which depends on the lattice constants a and c. The grain size, L, was obtained from the breadth, B, and the diffraction angle of the XRD peaks using the Sherrer equation, $L = 0.94\lambda / B\cos\theta$, where B is the full width at half maximum of the XRD peak at the diffraction angle 2θ. The results obtained are listed in Table 1 for comparison with the lattice constants of ZnO powder. The results reveal that the c/a ratio in films is smaller than that for the powder sample. This indicates the presence of lattice strain in the films. The annealing process reduces the strain and, hence, the c/a ratio approaches towards that for the powder sample. The influence of the annealing ambient on the relaxation of strain is evident from the results. As the c/a ratio increases towards its value for the powder sample, the grain size also increases by a factor of four in the range of 9 - 39 nm.

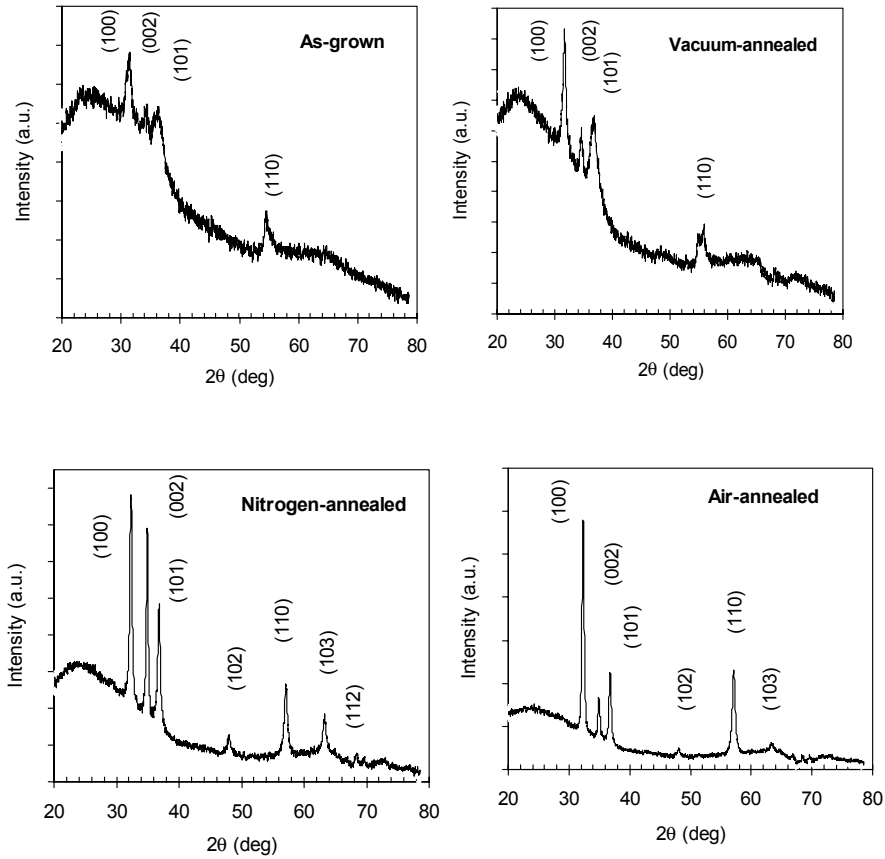

Fig. 3. XRD patterns for the as-grown and annealed films.

Table 1. Lattice constants, *a* and *c*, grain size, L, direct transition energy, E_d, and indirect transition energy, E_i, for the as-grown and annealed films

Sample	*a* (nm)	*c* (nm)	*c*/*a*	L (nm)	E_d (eV)	E_i (eV)
As-grown	0.3324	0.5181	1.5587	9	2.42	1.80
Vacuum-annealed	0.3277	0.5181	1.5810	10	3.04	1.50
Air-annealed	0.3210	0.5132	1.5988	23	3.18	1.72
Nitrogen-annealed	0.3211	0.5137	1.5998	39	3.26	1.80
Powder sample	0.3254	0.5263	1.6174			

Optoelectronic properties

Figure 4 depicts the optical transmittance spectra for the as-grown and annealed films. The transmittance of the as-grown film does not show a steep rise in the

vicinity of the band edge. This is due to the presence of excessive nitrogen impurities and the related structural defects as inferred from the poor crystallineity of the as-grown films (Fig. 3). The yellow-brown color of the as-grown film turns darker by annealing the film in vacuum. This is evident from the much lower transmittance of the respective plot in Figure 4 as compared to that for the as-grown film. This is in agreement with the XPS results, discussed above, which indicate that annealing in vacuum increases the concentration of elemental Zn in the film apparently due to the escape of oxygen. Annealing in nitrogen and in air improves the optical transmittance of the films in the visible region as a result of the improvement of the films crystallineity as evident from their XRD patterns.

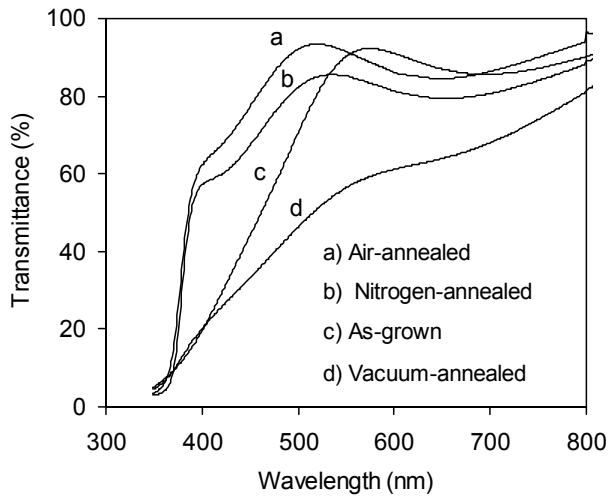

Fig. 4. Optical transmittance spectra for the as-grown and annealed films.

The as-grown and annealed films exhibited a reasonably good photoconductivity response in the visible region. Figure 5 shows the spectral response of photocurrent normalized to the incident photon flux R, for the as-grown and annealed films. For comparison, the spectral response of R for a nitrogen-free ZnO film is also shown. This film was sputter deposited using only argon as the sputtering gas. For this film the spectral response is entirely in the UV range (below 400 nm) as expected. The peak appearing in the plots in Figure 5 can be explained as it follows. As the incident wavelength is lowered toward the band edge wavelength, the optical absorption coefficient and the R value are both increased. As the absorption coefficient increases, the electron-hole pairs (EHP) are generated closer to the film surface. This enhances the recombination rate of the EHPs due to the effect of surface states and consequently R starts to decrease as the wavelength is lowered further below 360 - 380 nm. In contrast

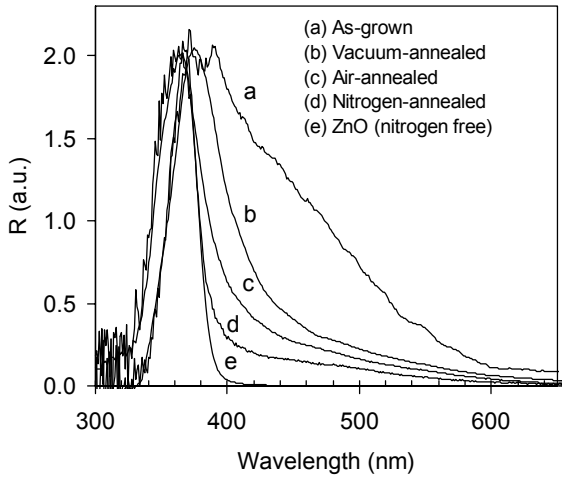

Fig. 5. The spectral response of the normalized photocurrent R, for the as-grown and annealed films. The plot for the undoped film is also shown

to the undoped ZnO, the spectral response of R for ZnO:N films is extended to the visible region. This implies that the photoconductivity response in the visible region is due to the presence of nitrogen-related defects in the doped films. The effect of annealing in different ambient on the extent of photocurrent response in the visible region is evident from Figure 5. The optical transitions involving the nitrogen-related defect levels and also the strain-related band gap contraction are both expected to contribute to the photocurrent response in the visible region. In the vicinity and above the involved transition energies (high absorption coefficients) R varies in proportion to the absorption coefficient. Therefore, the direct transition energies, E_d, or indirect transition energies, E_i, can be evaluated from the plots of $(RE)^2$ or $(RE)^{1/2}$ against the incident photon energy E, respectively (Kokaj & Rakhshani, 2004; Rakhshani, 2002). Figure 6 and its inset depict these plots which are constructed from the spectral response of the air-annealed film in Figure 5 (plot c). The horizontal intercepts of the line fits to these plots determine E_d = 3.18 eV and E_i = 1.72 eV. The former is assigned to the band gap energy and the latter to the ionization energy of a defect level. The results obtained for other films, using the same method, are summarized in Table 1. The ionization energy of the defect level varies in the range 1.50 - 1.80 eV (average, 1.71 eV) and does not show a correlation with the film c/a ratio. Since this energy level was not detected in the nitrogen-free ZnO film, it is attributed to the ionization energy of a nitrogen-related defect, likely $(N)_O$. A photoluminescence emission about 1.7 eV has also been observed in nitrogen doped ZnO films (Tarun *et al.*, 2011). Figure 7 shows the correlation between the E_d (band gap energy) and c/a values. The as-grown film has a

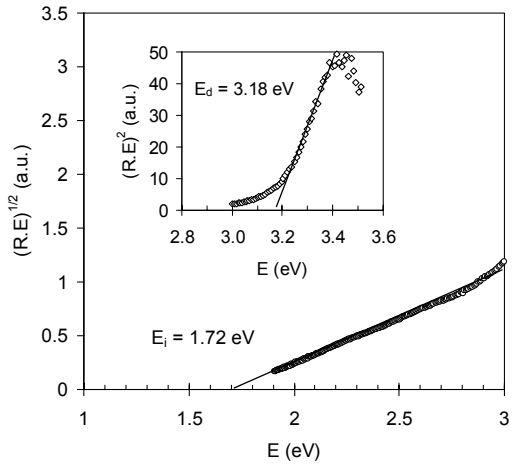

Fig. 6. Plots of $(RE)^{1/2}$ and $(RE)^2$ (inset) against the photon energy, E, for the air-annealed film. R is photocurrent normalized to the incident photon flux.

contracted band gap which is partially due to the strained unit cell where the c/a value is about 4% smaller than that for a nitrogen-free ZnO powder sample. In addition to the strain, other effects may also play a role. Nitrogen doping can lower the effective band gap of ZnO to about 2.2 eV due to the overlap of a nitrogen-related deep level with the valence band (Nakano *et al.*, 2005). Annealing apparently reduces the strain and also decreases the extent of this overlap. This leads to the increase of both c/a and E_d values toward their respective values for the ZnO powder sample. Obviously, the extent of the relaxation of band gap narrowing and strain by annealing depends on the annealing ambient.

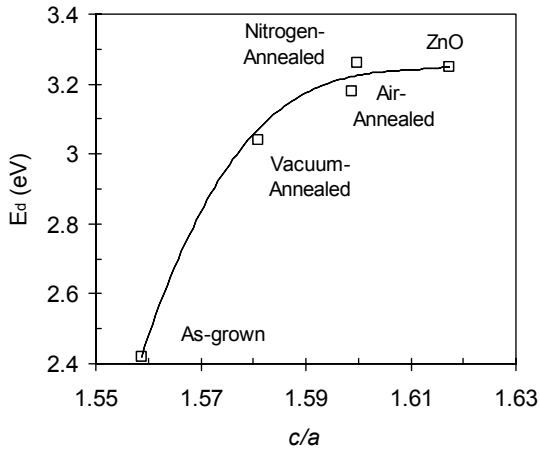

Fig. 7. Direct optical transition energy E_d, against the ratio of lattice constants, c/a.

Light-emitting homojunction diodes

The density and type of charge carriers in films annealed in nitrogen and in air were determined by Hall-effect measurement. These samples were annealed for 60 minutes at 500 °C. The nitrogen-annealed sample showed n-type conductivity with an electron density of 7.0×10^{14} cm^{-3} and electron mobility of 9.7 $cm^2V^{-1}s^{-1}$. The air-annealed sample showed p-type conductivity with the hole density and mobility of 5.5×10^{15} cm^{-3} and 0.73 $cm^2V^{-1}s^{-1}$, respectively. The conversion of ZnO:N to p-ZnO is due to the net density of donor-type defects such as $(N_2)_O$, V_O and Zn_i to fall below the density of shallow acceptor levels. This occurs as a result of the out diffusion of N_2 from $(N_2)_O$ defects. Li *et al.* (2008) have demonstrated that for a 30-minute annealing time, the hole density increases from 3.25×10^{15} cm^{-3} to 2.85×10^{18} cm^{-3} by lowering the annealing temperature from 600 °C to 400 °C. Similar results have also been reported by Wang *et al.* (2003) which indicate that oxidation at 400- 450 °C yields a hole density in the range $(1\text{-}6) \times 10^{17}$ cm^{-3}, two orders of magnitude greater than that in samples oxidized at 500 °C. The annealing time is also expected to play an important role in the conversion process. For the fabrication of homojunction devices, as described below, we used a low oxidation temperature (400 °C) and a short annealing time (5 min) to convert the ZnO:N films deposited on stainless steel to p-ZnO. Due to the high conductivity of the substrate, the density of holes in the converted film could not be determined by Hall-effect measurement. Instead, it was measured as 1.5×10^{17} cm^{-3} from the capacitance-voltage characteristic of a homojunction diode fabricated on the converted p-ZnO film.

For the preparation of homojunction devices, a 100-nm ZnO:N film was sputter deposited on a pre-cleaned flexible stainless steel (SS) substrate. The sample was annealed in air (400°C, 5 min) for the conversion of ZnO:N layer to p-ZnO. An intrinsically n-ZnO film with a thickness of 820 nm was electrodeposited on top of the p-ZnO film from a 100-mM zinc nitrate solution at 80 °C. Electrodeposition was carried out at a cathode (SS coated with p-ZnO) potential of -1.0 V with respect to a saturated silver chloride reference electrode. The deposition procedure has been described elsewhere and the electron density in electrodeposited ZnO films has been measured to be in the range $(1\text{-}5) \times 10^{17}$ cm^{-3} (Rakhshani, 2010). The device structure, the surface morphology of the p-ZnO film grown on SS and the cross section view of the electrodeposited n-ZnO film are shown in the inset of Figure 8. Both films have a compact structure as is evident from Figure 8. Circular contacts of gold (diameter 2 mm, thickness 30 nm) were deposited on n-ZnO by thermal evaporation. This was followed by a 10-minutes air annealing (400 °C) to remove the hydroxide compounds from the electrodeposited film. The IV plot in Figure 8 shows a rectification factor (ratio of forward to reverse current) of 230 (± 3 V) for a typical device.

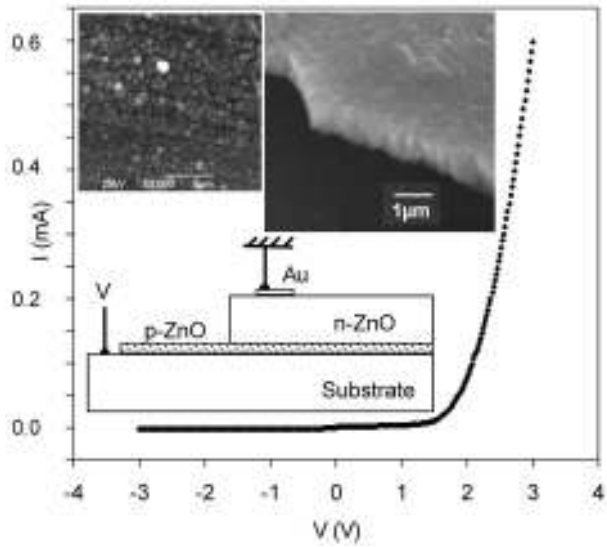

Fig. 8. The current-voltage plot of a homojunction diode prepared on stainless steel substrate. Insets show the device configuration, SEM views from the surface of p-ZnO and cross section of electrodeposited n-ZnO films.

The forward current corresponds to the positive polarity of the substrate bias, indicating the formation of a p-n junction between the p-ZnO and the top n-ZnO layers. The nature of the junction between the gold contact and the n-ZnO layer was examined in devices prepared without the conversion of ZnO:N layer to p-ZnO. These devices showed a weak IV rectification (factor of 2 to 3) with the forward current corresponding to the negative polarity of the substrate, opposite to the case shown in Figure 8. Therefore, the relatively high rectification factor and the correct polarity of the forward current in Figure 8 verify the formation of a p-n homojunction device. The voltage dependence of the capacitance of a p-n junction with a uniform doping profile is expressed by $C^{-2} = 2(V_o - V)/q\varepsilon A^2N$, where $N = N_aN_d/(N_a + N_d)$ (Neamen, 2003). Here, V_o is the junction built-in potential, q is the electronic charge, $\varepsilon = 7.1x10^{-11}$ F/m is the permittivity of ZnO and $A = 3x10^{-6}$ m^2 is the device active area. N_a and N_d are the uncompensated density of acceptors and donors in the p-ZnO and n-ZnO films, respectively. A plot of C^{-2} against V is expected to yield a straight line with a horizontal intercept V_o and a slope from which N can be evaluated. The CV plot of a device measured at 100 kHz is shown in Figure 9. The straight line fit to the data points measures $V_o = 0.37$ V and $N = 1.3x10^{17}$ cm^{-3}. The measured values of these two parameters varied in the range 0.4 - 1.0 V and (1-2)$x10^{17}$ cm^{-3} among several devices examined. The donor density in the n-ZnO

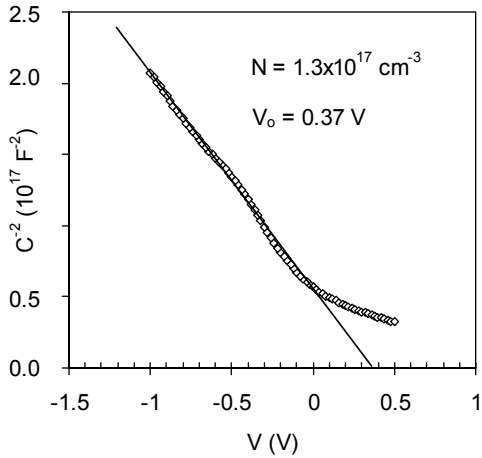

Fig. 9. The capacitance-voltage plot of a homojunction diode.

layer was determined as N_d = (1-5)x10^{17} cm^{-3} from the CV characteristics of the n-ZnO films electrodeposited on p^+-Si substrate (Rakhshani, 2010). Hall-effect measurement cannot be performed on electrodeposited films due to their conducting substrates. From the average value of N_d (= 3x10^{17} cm^{-3}) and the measured N value (= 1.5x10^{17} cm^{-3}), the acceptor density in the converted p-ZnO films was determined as N_a = 1.5x10^{17} cm^{-3}. This value is greater than N_a = 5.5x10^{15} cm^{-3} measured for p-ZnO films on glass which were converted at a higher temperature (500 °C) as discussed above. This observation is consistent with the other reports (Li *et al.*, 2008; Wang *et al.*, 2003).

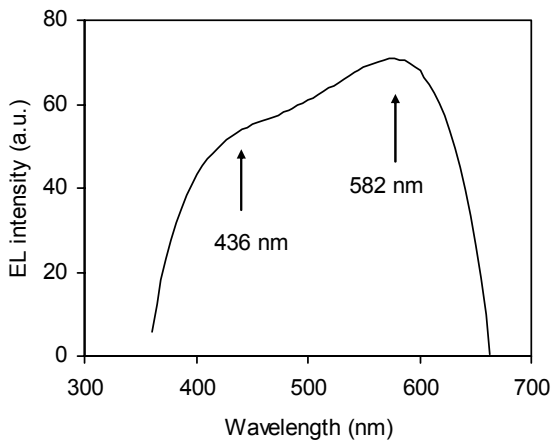

Fig. 10. The spectrum of light emitted from a homojunction diode under a forward bias of 3 V at 300 K.

Figure 10 depicts the EL spectrum of a device under the forward bias. The spectrum covers the visible and part of the UV range (363 - 400 nm). The emission spectrum is formed from two broad peaks centered at 436 nm (2.84 eV) and 582 nm (2.13 eV). Taking the band gap as 3.37 eV, the 436-nm emission can be assigned to a radiative transition from the prominent E_4 defect level in the n-ZnO layer to the valence band. The E_4 defect level, with an unknown origin, is located 0.57 eV below the conduction band (CB) of ZnO (Auret *et al.*, 2002). The emission at 582 nm represents a transition from the CB to the doubly-ionized oxygen-vacancy defect level in the n-ZnO layer. This defect level is located 2.1 - 2.2 eV below the CB of n-ZnO (Rakhshani, 2008). These two emissions have also been observed in the EL spectrum of p-i-n heterojunction devices fabricated from electrodeposited n-ZnO films (Rakhshani, 2010). Electroluminescence from other heterojunction devices fabricated from electrodeposited n-ZnO and p-polymers has also shown a defect-related broad emission covering the entire visible region (Konenkamp *et al.*, 2007). These heterojunction devices as well as the homojunction devices discussed here do not show a band-to-band EL peak at 365-380 nm. This is apparently due to the dominant role of the band gap defect levels in the vicinity of the junction.

SUMMARY AND CONCLUSIONS

Thin films of ZnO:N were deposited on glass substrate by reactive sputtering using a Zn target. The N/(Zn + O) atomic ratio is ~ 0.07 in the as-grown films. Annealing (500 °C, 60 min) reduces this ratio to ~ 0.007. Nitrogen is incorporated in the films in the form of Zn_3N_2, donor-type $(N_2)_O$ defects, acceptor-type $(N)_O$ defects and organic compounds (N-C bonds). Annealing in nitrogen ambient slightly increases the density of $(N_2)_O$ and reduces appreciably the density of $(N)_O$ defects. Annealing in vacuum increases the density of the elemental Zn, the $(N_2)_O$ and V_O defects. Air annealing reduces the density of $(N_2)_O$ donor-type defects below that for the shallow-acceptor complex defects, leading to the conversion of films to p-ZnO.

The as-grown ZnO:N films have a hexagonal structure with a strained unit cell where the ratio of the lattice constants, c/a, is 4% smaller than that for the ZnO powder. Annealing reduces the lattice strain and increases the c/a ratio. The extent of the strain relaxation varies with the annealing ambient. The grain size increases from 9 nm in the as-grown films to 39 nm in the nitrogen-annealed films.

The optical transmittance decreases by annealing the films in vacuum. Annealing in air or in nitrogen improves the films transmittance at wavelengths below 600 nm. The as-grown and annealed films show good photoconductivity response in the visible region most likely due to the involvement of the nitrogen-related defect level with ionization energy of 1.71 eV. The direct band gap varies from 2.42 eV for the as-grown film to 3.26 eV for the film annealed in nitrogen.

Homojunction devices prepared from electrodeposited n-ZnO and nitrogen-doped films converted to p-ZnO at 400 °C showed a diode-type IV characteristic. From the CV characteristics of these devices the acceptor density in p-ZnO films was measured as 1.5×10^{17} cm^{-3}. These devices showed defect-related EL in a wide wavelength range covering the visible and part of the UV region. The active defects in the light emission process are the ZnO prominent E_4 and the doubly ionized V_O defects.

ACKNOWLEDGEMENT

We thankfully acknowledge the support of Kuwait University under the research projects SP03/09, SP01/06 and Science General Facility projects.

REFERENCES

Auret, F. D., Goodman, S. A., Legodi, M. J., Meyer, W. E. & Look, D. C. 2002. Electrical characterization of vapor-phase-grown single-crystal ZnO. Applied Physics Letters **80**: 1340.

Djurisic, A. B., Leung, Y. H., Tam, K. H., Hsu, Y. F., Ding, L., Ge, W. K., Zhong, Y. C., Wong, K. S., Chan, W. K., Tam, H. L., Cheah, K. W., Kwok, W. M. & Phillips, D. L. 2007. Defect emissions in ZnO nanostructures. Nanotechnology **18**: 095702.

Fons, P., Tampo, H., Kolobov, A. V., Ohkubo, M., Niki, S., Tominaga, J., Carboni, R., Boscherini, F. & Friedrich, S. 2006. Direct observation of nitrogen location in molecular beam epitaxy grown nitrogen-doped ZnO. Physical Review Letters **96**: 045504.

Kato H., Yamamuro T., Ogawa A., Kyotani C. & Sano M. 2011. Impact of Mixture Gas Plasma of N_2 and O_2 as the N source on ZnO-based ultraviolet light-emitting diodes fabricated by molecular beam epitaxy. Applied Physics Express **4**: 091105.

Khan, W. S. & Cao, C. 2010. Synthesis, growth mechanism and optical characterization of zinc nitride hollow structures. Journal of Crystal Growth **312**: 1838-1843.

Kokaj, J. & Rakhshani, A. E. 2004. Photocurrent spectroscopy of solution-grown CdS films annealed in $CdCl_2$ vapour. Journal of Physics D: Applied Physics **37**: 1970-1975.

Konenkamp, R., Word, R. C., Dosmailov, M., Meiss, J. & Nadarajah, A. 2007. Selective growth of single-crystalline ZnO nanowires on doped silicon. Journal of Applied Physics **102**: 056103.

Li, B. S., Liu, Y. C., Zhi, Z. Z., Shen, D. Z., Lu, Y. M., Zhang, J. Y., Fan, X. W., Mu, R. X. & Henderson, Don. O. 2003. Optical properties and electrical characterization of p-type ZnO thin films prepared by thermally oxidizing Zn_3N_2thin films. Journal of Materials Research **18**: 8-13.

Li, L., Shan, C. X., Li, B. H., Yao, B., Zhang, J. Y., Zhao, D. X., Zhang, Z. Z., Shen, D. Z., Fan, X. W., Lu, Y. M. 2008. The compensation source in nitrogen doped ZnO. Journal of Physics D: Applied Physics **41**:245402.

Liu J. S., Shan C. X., Shen H., Li B. H., Zhang Z. Z., Liu L., Zhang L. G. & Shen D. Z. 2012. ZnO light-emitting devices with a lifetime of 6.8 hours. Applied Physics Letters **101**: 011106.

Liu, W. W., Yao, B., Zhang, Z. Z., Li, Y. F., Li, B. H., Shan, C. X., Zhang, J. Y., Shen, D. Z. & Fan, X. W. 2011. Doping efficiency, optical and electrical properties of nitrogen-doped ZnO films. Journal of Applied Physics **109**: 093518.

Look, D. C. 2005. Electrical and optical properties of p-type ZnO. Semiconductor Science and Technology **20**: S55-S61.

Lyons J. L., Janotti A. & Van de Walle C. G. 2009. Why nitrogen cannot lead to p-type conductivity in ZnO. Applied Physics Letters **95**: 252105.

Nakahara K., Akasaka S., Yuji H., Tamura K., Fujii T., Nishimoto Y., Takamizu D., Sasaki A., Tanabe T., Takasu H., Amaike H., Onuma T., Chichibu S. F., Tsukazaki A., Ohtomo A. & Kawasaki M. 2010. Nitrogen doped $Mg_xZn_{1-x}O$/ ZnO single heterostructure ultraviolet light-emitting diodes on ZnO substrates. Applied Physics Letters **97**: 013501.

Nakano, Y., Morikawa, T., Ohwaki, T. & Taga, Y. 2005. Deep level characterization of N-doped ZnO films prepared by reactive magnetron sputtering. Applied Physics Letters **87**: 232104.

Nakano, Y., Morikawa, T., Ohwaki, T. & Taga, Y. 2006. Electrical characterization of p-type N-doped ZnO films prepared by thermal oxidation of sputtered Zn_3N_2 films. Applied Physics Letters **88**: 172103.

Neamen, D. A. 2003. Semiconductor Physics and Devices: Basic Principles. McGraw Hill, New York. Pp 252.

Nunez, C. G., Pau, J. L., Hernandez, M. J., Cervera, M., Ruiz, E. & Piqueras, J. 2012. On the zinc nitride properties and the unintentional incorporation of oxygen. Thin Solid Films **520**: 1924-1929.

Özgür,Ü., Alivov, Ya. I., Liu, C., Teke, A., Reshchikov, M. A., Doğan, S., Avrutin, V., Cho, S. -J. & Morkoçd, H. 2005. A comprehensive review of ZnO materials and devices. Journal of Applied Physics **98**: 041301.

Paniconi, G., Stoeva, Z., Smith, R. I., Dippo, C. P., Gallagherd, B. L. & Gregory, D. H. 2008. Synthesis, stoichiometry and thermal stability of Zn_3N_2 powders

prepared by ammonolysis reactions. Journal of Solid State Chemistry **181**: 158-165.

Pearton, S. J., Norton, K. I., Heo, Y. W. & Steiner, T. 2003. Recent progress in processing and properties of ZnO. Superlattices and Microstructures **34**: 3-32.

Perkins, C., Lee, S. H., Lee, X., Asher, S. E. & Coutts, T. J. 2005. Identification of nitrogen chemical states in N-doped ZnO via x-ray photoelectron spectroscopy. Journal of Applied Physics **97**: 034907.

Qureshi, A., Shah, S., Pelagade, S., Singh, N. L., Mukherjee, S., Tripathi, A., Despande, U. P. & Shripathi, T. 2010. Surface modification of polycarbonate by plasma treatment. Journal of Physics: Conference Series **208**: 012108.

Rakhshani, A. E. 2002. Optoelectrical properties of electrodeposited $Cd_xHg_{1-x}Te$ with a bandgap energy of 1.35 eV. Semiconductor Science and Technology **17**: 924-930.

Rakhshani, A. E. 2008. Optical and electrical characterization of well-aligned ZnO rods electrodeposited on stainless steel foil. Applied Physics A **92**: 303-308.

Rakhshani, A. E. 2010. Optoelectronic properties of p-n and p-i-n heterojunction devices prepared by electrodeposition of n-ZnO on p-Si. Journal of Applied Physics **108**: 094502.

Sun F., Shan C. X., Li B. H., Zhang Z. Z., Shen D. Z., Zhang Z. Y. & Fan D. 2011. A reproducible route to p-ZnO films and their application in light-emitting devices. Optics Letters **36**: 499-501.

Tarun M. C., Zafar Iqbal M. & McCluskey M. D. 2011. Nitrogen is a deep acceptor in ZnO. AIP Advances **1**: 022105.

Wang, C., Ji, Z., Liu, K., Xiang, Y., & Ye, Z. 2003. p-Type ZnO thin films prepared by oxidation of Zn_3N_2 thin films deposited by DC magnetron sputtering. Journal of Crystal Growth **259**: 279-281.

Wang, D., Liu, Y. C., Mu, R., Zhang, J. Y., Lu, Y. M., Shen, D. Z. & Fan, X. W. 2004. The photoluminescence properties of ZnO:N films fabricated by thermally oxidizing Zn_3N_2 films using plasma-assisted metal-organic chemical vapour deposition. Journal of Physics: Condensed Matter **16**: 4635-4642.

Watanabe, F., Shirai, H., Fujii, Y. & Hanajiri, T. 2011. Rapid thermal annealing of sputter-deposited ZnO/ZnO:N/ZnO multilayered structures. Thin solid Films **520**: 3729-3735.

Yang, T., Zhang, Z., Li, Y., Lv, M., Song, S., Wub, Z., Yan, J. & Han, S. 2009. Structural and optical properties of zinc nitride films prepared by rf magnetron sputtering. Applied Surface Science **255**: 3544-3547.

Zhang, J. P., Zhang, L. D., Zhu, L. Q., Zhang, Y., Liu, M. & Wang, X. J. 2007. Characterization of ZnO:N films prepared by annealing sputtered zinc oxynitride films at different temperatures. Journal of Applied Physics 102:114903.

Zong, F., Ma, H., Xue, C., Du, W., Zhang, X., Xiao, H., Ma, J. & Ji, F. 2006. Structural properties of zinc nitride empty balls. Materials Letters 60: 905-908.

Zou, C. W., Chen, R. Q. & Gao, W. 2009. The microstructures and the electrical and optical properties of ZnO:N films prepared by thermal oxidation of Zn_3N_2 precursor. Solid State Communications 149: 2085-2089.

Submitted : *18/12/2012*
Revised : *10/04/2013*
Accepted : *15/04/2013*

تحضير وتوصيف رقاقات نحيفة من أكسيد الزنك المطعم بالنيتروجين وصمام الكتروني ثنائي متجانس منطقة الإلتقاء السطحية

***علي راخشاني و **علي بو مجداد و * يحيى كوكاج و *سوني توماس**

*قسم الفيزياء و **قسم الكيمياء ، كلية العلوم، جامعة الكويت
ص.ب: 5969 صفاة 13060 كويت

خلاصة

تم تحضير رقائق أكسيد الزنك المطعم بعنصر النيتروجين عبر تقنية ترسيب المواد وهي في الحالة الغازية باستخدام قطب من الزنك. تم بحث تأثير المعالجة الحرارية في أجواء مختلفة على: مكونات الرقائق، حالة الروابط الكيميائية، التركيب الكيميائي، النفاذية البصرية، وكذلك التوصيل الفوتوني. لقد وجد أن الرقاقة وقبل معالجتها الحرارية مكونة من حبيبات ذات حجم 9 نانومتر، وتبين أيضاً أن وحدة الخلية متأثرة وليست طبيعية. المعالجة الحرارية تزيل هذا التأثير على وحدة الخلية وتزيد حجم الحبيبات المكون للرقاقة إلى 39 نانومتر. المعالجة الحرارية وجدت أيضاً أنها تزيد الفجوة بين إلكترونات التكافؤ وإلكترونات التوصيل من قيمة 2,42 إلكترون فولت إلى 3,26 فولت إلكتروني. تبين النتائج أن الرقائق الغير المعالجة وكذلك المعالجة حرارياً لهم خواص توصيل فوتوني في منطقة الضوة المشاهد، وهذا يعود جزئياً إلى العيوب التي تسببت بها ذرات النيتروجين ذات طاقة تأين تساوي 1,71 فولت إلكتروني. تم تحويل رقائق أكسيد الزنك الغير معالجة حرارياً من نوع n إلى نوع p عن طريق المعالجة الحرارية في وجود الهواء. كما تم استخدام رقائق أكسيد الزنك من النوع n والمحول إلى النوع p في تصنيع الصمام الثنائي المتجانس الباعث للضوء. لقد وجد أن الصمامات الثنائية المحضرة تمتلك معامل تصحيح تيار –فولت ذو قيمة معقولة وجيدة ولها صفات انبعاثات ضوئية كهربائية في منطقة الفوق بنفسجية. من السعة الكهربائية لمنطقة الالتقاء لهذه الصمامات الثنائية تبين أن كثافة الثقوب في رقاقات أكسيد الزنك من النوع p والتي تم تنميتها على مادة الإستيل (الحديد المكربن) كانت تساوي $1.5 \times 10^{17} \mathrm{cm}^{-3}$.

مجلة دراسات الخليج والجزيرة العربية

مجلة علمية فصلية محكمة تصدر عن مجلس النشر العلمي - جامعة الكويت
صدر العدد الأول منها في يناير عام ١٩٧٥م

ترحـب المجلة بنشر البحوث والدراسات العلمية المتعلقة بشؤون منطقة الخليج والجزيرة العربية في مختلف علوم البحث والدراسة .

ومن أبوابها

- البحوث العربية.
- البحوث الإنجليزية.
- عرض الكتب ومراجعتها .
- البيبلوجرافيا العربية.
- ملخصات الرسائل الجامعية: ماجستير - دكتوراه.
- التقارير: مؤتمرات - ندوات

الاشتراكات

ترسل قيمة الاشتراك مقدماً بشيك لأمر - جامعة الكويت
مسحوب على أحد المصارف الكويتية

داخل دولة الكويت : للأفراد : 3 دنانير - للمؤسسات : 15 ديناراً
الـدول الـعـربـيـة : للأفراد : 4 دنانير - للمؤسسات : 15 ديناراً
الدول الغير عربية : للأفراد : 4 دنانير - للمؤسسات : 15 ديناراً

توجه جميع المراسلات باسم رئيس تحرير مجلة دراسات الخليج والجزيرة العربية

Tel.: (+965) 24833213 - 24984066 - 24984067 Fax: (+965) 24833706 P.O. Box 17073 Al-Khaldiah, 72451 Kuwait
www.pubcouncil.kuniv.edu.kw/jgaps E - mail : jgaps@ku.edu.kw
www.ku.edu.kw